738 J. Chem. Eng. Data **1995,** *40,* 738–745

Infinite Dilution Activity Coefficients of Acetone in Water. A New Experimental Method and Verification

Roger P. Hartwick and Colin S. Howat*

Kurata Thermodynamics Laboratory, Department of Chemical & Petroleum Engineering, University of Kansas, Lawrence, Kansas 66045-2223

The requirements for the removal of volatile organic compounds in processes are becoming more stringent. Process designs to accomplish the removal of volatile organic compounds require knowledge of the infinite dilution behavior in water. This can be estimated by extrapolating finite phase equilibrium data into the infinite dilution region. However, this is solution model dependent; i.e., different models describing the same acetone + water data predict γ^∞ which differ by a factor of 3. The consequence is predicted tray requirements up to 3 times different for the same separation. More reliable infinite dilution activity coefficients based on experimental data are required for reliable process design. One method is to estimate the slope $(\mathrm{d}P/\mathrm{d}x)_{x=0}$ by measuring $(\mathrm{d}P/\mathrm{d}x)_{x>0}$ at low compositions and extrapolating to infinite dilution. Ebulliometric methods are subject to temperature gradients and pressure fluctuations. Conventional static methods suffer from the presence of noncondensable chemicals. Both affect the slope and, thus, γ^∞ estimates. This paper presents a modified static method. A large, calibrated vapor space minimizes the impact of noncondensable chemicals. The degassed solute is micrometered incrementally into the cell containing water. Experimental design methods testing the impact of the number and volume of the metered solute verify the accuracy and precision of the resultant γ^∞ values. Results for acetone are reported and compared to literature values. The comparison verifies the validity of the experimental method.

Introduction

Designers frequently choose to work with solution model parameters which have been developed through the analysis of data over the whole range of composition. While this is acceptable for conventional design of distillation and other mass transfer processes, the practice leads to unreliable processes when they operate in the infinite dilution region. A typical example is in the design of separation equipment to remove volatile organic compounds from waste water. Hartwick and Howat (1993) have shown that extrapolation of activity coefficients into the infinite dilution region using solution models introduces a systematic error in the estimation of the phase equilibria. This bias translates into an error of 50% in the estimated number of trays needed to remove volatile organic compounds from waste water. Such uncertainty can easily lead to grossly inefficient or flooded towers. While other technologies are available for purifying waste water, most rely on the underlying thermodynamics. The uncertainty in the design of distillation equipment resulting from misestimating the thermodynamics also applies to these other technologies. Consequently, accurate values of the infinite dilution behavior are required for reliable process design. These values come from measurement of the phase equilibria at infinite dilution.

Experimental measurement of the infinite dilution phase behavior leading to estimates for γ^∞ is generally done in four ways (Abbott, 1986): (1) ebulliometry, (2) gas/liquid elution chromatography, (3) head space chromatography, and (4) static total pressure. Historically, ebulliometric methods have been the most common, but the latter methods have gained favor.

Ebulliometric methods involve boiling the mixture in an isothermal or isobaric still. The vapors rising from the liquid are condensed and returned to the boiling chamber and again mixed with the liquid. Constant temperature and pressure over time are used to conclude that equilibrium has been reached inside the entire still. The liquid and vapor phases may be sampled and analyzed to obtain the composition of the respective phases. However, sample handling in wide-boiling systems has proved difficult and can result in substantial errors in composition when analyzing the fluids. Techniques have been developed to measure temperature to within 0.001 K, but temperature gradients in the cell are common. Methods have been developed to accurately measure pressure, but pressure fluctuations are typically observed when the relative volatility between the two components is large. Large relative volatilities at very low compositions are typical in volatile organic compound + water systems. Consequently, the pressure fluctuations, temperature gradients, and sampling difficulties are to be expected. These lead to inaccurate experimental measurements unless extreme care is taken.

Gas/liquid elution chromatography is used to determine infinite dilution activity coefficients by measuring the elution time of the dilute species (solute) in an inert carrier stream through a column composed of the abundant species (solvent). In this method the infinite dilution activity coefficient is inversely related to the elution time. The dilutor method uses chromatography to analyze the composition of an inert gas stream that has been bubbled through the solution to be tested. Changes in the composition of the solution over time are measured with the chromatograph, and the differential equations describing the change with time can be integrated to find the value of the infinite dilution activity coefficients (Leroi and Masson, 1977).

Head space chromatography allows direct sampling with a chromatograph (Shaw and Anderson, 1983). The liquid composition is well known, and in conjunction with the measured vapor composition, the activity coefficient can be calculated. The total pressure is not measured. The vapor sample may be contaminated with noncondensable

0021-9568/95/1740-0738$09.00/0 © 1995 American Chemical Society

chemicals, e.g., nitrogen and oxygen; however, this method does not require that the sample be noncondensable chemical free. This method does not suffer from the nonequilibrium characteristics of the ebulliometric method, nor does it require special chromatographic columns and complex analysis that are required by elution chromatographic methods. It is likely that this method is suitable over a wider range of relative volatilities than the other methods. However, the measurement of composition is typically more complicated than the measurement of pressure. The static total pressure method has advantages in that the vapor composition does not have to be measured.

The static total pressure method involves metering liquid samples into an evacuated cell, allowing the fluids to come to equilibrium at a constant temperature, and measuring the resultant pressure. The liquid may be sampled, but vapor samples, unless extremely small, will disrupt the equilibrium; therefore, it is very rarely done (Abbott, 1986). The major drawback of static methods is the requirement that the samples be thoroughly degassed. If this is not done, the dissolved gases will distort the bubble point pressure measurement, thus affecting the estimate of the slope of the pressure as solute concentration approaches zero. Degassing can be accomplished by distillation of the liquid under vacuum, multiple freezing–evacuating–thawing cycles of the compound, or sublimation of the compound under vacuum. Repeated measurements of the pressure of the pure component can be used to check the completeness of the degassing procedure. Analysis of the phases is rarely performed; instead, gravimetric or volumetric metering is used to calculate the overall composition, and the data analysis procedure must calculate compositions for each phase. Overall, the static method is the most accurate way to measure the phase behavior of very volatile systems such as those encountered in volatile organic compound + water systems (Rogalski and Malanowski, 1980).

Experimentalists at the Kurata Thermodynamics Laboratory have had extensive experience with the total pressure (static) method applied to measuring the phase behavior in the finite composition region (e.g., Shanker et al., 1981; Howat and Swift, 1984; Laird and Howat, 1990). The method is similar to that of Tomlins and Marsh (1976). Equipment has been designed, built, and tested to accurately meter materials, control temperatures, and measure pressure. In this work, a modified static method has been developed to measure the phase behavior of dilute solutions which minimizes the effect of noncondensable chemicals in the samples. This modified procedure draws upon our experience in static measurements, experimental design, and data analysis. The purpose of this paper is to introduce the modified static method for the experimental determination of infinite dilution phase behavior of volatile organic compounds in water. The veracity of this method is proven through experimental design simulations and experimental verification.

Experimental Equipment

The experimental equipment is a derivative of that developed by Howat (1983). The schematic of the equipment as it is currently configured is shown in Figure 1. The equipment contains positions for six precision bore glass tubes, four of which (C3–C6) are shown, with inside diameters accurate to 0.005 mm. Cells can be connected to the top and bottom manifolds or can be connected to one manifold and to a piston drive. In the current version, two 8 mm cells of variable volume have mechanically driven pistons which enter the bottom of the cells (C3 and C4). A 2 mm diameter microcell (C5) is used for accurate metering at low compositions. The fourth cell (C6) is of fixed volume. The cell and manifold assembly is enclosed in a well-insulated, constant temperature bath. The upper manifold shown in Figure 1 is connected to an external manifold which in turn is connected to vacuum, a liquid supply, and the atmosphere. Temperature is controlled to ±0.02 K and measured to ±0.01 K. Temperature control is effected with a Bayley Model 250 temperature controller in conjunction with a platinum resistance thermometer. Two Yellow Springs platinum RTDs calibrated against an NBS standard are used to measure cell temperatures and bath gradients. Pressures are measured using a Paroscientific pressure transducer (model 2100-AS-002, range 0–100 psia) which is calibrated and repeatedly checked against an NBS-calibrated Ruska dead weight balance. The transducer is held in a separate isothermal bath with the set point slightly above the cell temperature to minimize condensation in the transducer. Since the transducer calibration is a function of temperature, the calibration was performed at the transducer temperature. Pressure measurement is accurate to ±0.08 kPa. Precision adjustment of the pistons results in accurate metering of chemicals from any of the variable volume cells (C3–C5) into C6. Height measurements are made using a cathetometer accurate to 0.05 mm.

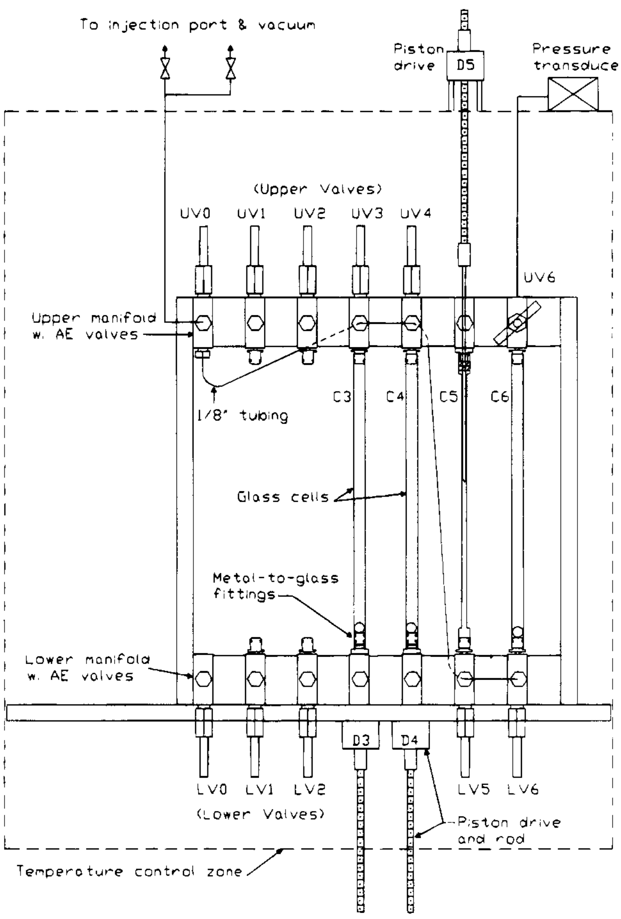

Figure 1. Experimental apparatus: UV = upper manifold valve; LV = lower manifold valve; C = glass cell; D = piston drive; AE = autoclave engineers modified valve.

The following describes the techniques used to prepare a mixture. The equipment is evacuated for an extended period (>48 h, typically). Cells C3, C4, and C6 are then repeatedly charged and flushed with deionized water to remove residual volatile organic compounds and noncondensable chemicals. Water is then charged to the manifold and one of the 8 mm variable volume cells, e.g., C3. After temperature equilibrium is established, the water (which had been degassed outside of the bath) is subjected to two extended boiling periods to reject residual noncondensable chemicals. Temperature equilibrium is reestablished. The desired amount of water is then metered into C6. The initial piston height is measured with the water in C3 and the manifold and UV3 open. The valve to C6 (LV6) is cracked, the piston in C3 is driven upward until the approximate height is reached, and LV6 is closed. After temperature equilibrium is reestablished, the piston height is measured accurately. The displacement of the piston translates into the volume of water metered and, through density, the mass of water metered. Temperature equilibrium is reestablished, and the vapor pressure of water is measured as a final check on purity. UV3 is closed, and the manifold is evacuated. C4 and the manifold are flushed with the solute of interest. The solute is then charged to C4. It is subjected to repeated boiling and holding periods to remove residual noncondensable chemicals not removed prior to charging. Temperature equilibrium is reestablished, the solute is metered to C5, and C4 is isolated from the manifold by closing UV4. C5 can be used to meter very small quantities to C6. This metering is done incrementally. After each increment, the contents of C6 are stirred using the magnetically driven stainless steel ball shown in C6 and equilibrium is established. The pressure is then measured. The liquid volume of the mixture in C6 is kept sufficiently small to minimize the effect of the noncondensable chemicals. The result is a traverse of overall composition, z, and pressure, P. With appropriate interpretation, the data can be translated into a $P-x$ traverse and $(\partial P/\partial x_1)_T$ can be calculated.

The purity of water used in this experiment is 99.9+%. The water was treated by reverse osmosis filtration to remove impurities before use. The acetone was Fisher spectrophotometric grade (99.7 mol %) stored over molecular sieves to remove the water.

Analysis

The experimental method is based on that of Howat (1983) with modifications made to the equipment and methods to allow smaller increments to be metered into C6. The infinite dilution activity coefficients are found from the $P-x$ traverse using a modified Gautreaux and Coates (1955) method. Prior to making any measurements, the accuracy and precision criteria of γ^∞ required for reliable process design are established. The experiment is then designed, i.e., the number and size of the chemical increments are determined, using Monte Carlo simulation to obtain that precision. The experimental design methods of Howat and Swift (1983) are used to develop the appropriate experimental design and to analyze the impact of potential problems which would result in systematic errors in the γ^∞ values.

The equation developed by Gautreaux and Coates relates the infinite dilution activity coefficient to the partial derivative of pressure with respect to liquid composition:

$$\gamma_1^\infty = (P/P_1^0)\{1 + (1/P)(\partial P/\partial x_1)_T^{x=0}\} \qquad (1)$$

The accuracy of the estimate of γ^∞ depends upon the accuracy of the estimate of the partial derivative. If the $P-x$ relationship is known, pressure can be described as a function of composition and the partial derivative can be determined by differentiation. The $P-x$ relationship is typically nonlinear, resulting in systematic errors if it is extrapolated to $x = 0$. An alternative is the auxiliary description developed by Ellis and Jonah (1962). They use a term measuring the departure from ideality:

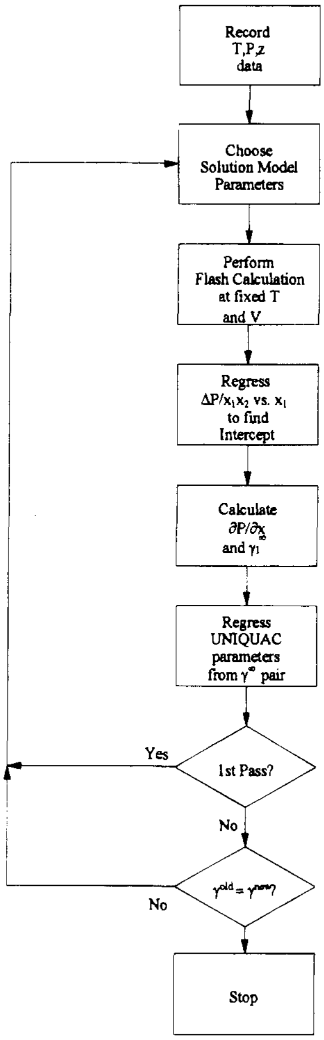

Figure 2. Procedure to calculate limiting activity coefficients from total pressure data.

$$\Delta P = P - x_1P_1^0 - x_2P_2^0 \qquad (2)$$

This has a useful property in the limit as $x_1 \to 0$:

$$(\Delta P/x_1x_2)_{x_1=0} = (\partial P/\partial x_1)_{x_1=0} - P_1^0 + P_2^0 \qquad (3)$$

The partial derivative is estimated by determining the intercept of the departure function divided by x_1x_2. The slope of $\Delta P/x_1x_2$ is linear in many cases (Maher and Smith, 1979).

Equation 3 requires that the pressure, temperature, and liquid composition be well known as $x_1 \to 0$. However, the volumetric metering provides accurate knowledge of the bulk cell composition. The large vapor space designed into the experiment to minimize the effect of residual noncondensable chemicals coupled with the volatility of the solute results in the liquid composition being different from the bulk composition. Figure 2 provides a method for calculating the liquid composition, x, from the bulk composition, z.

In order for this system to satisfy the phase rule, two independent, intensive variables must be set. The equilibrium cell is at a fixed temperature and has a fixed volume and a fixed mass of each chemical species. This

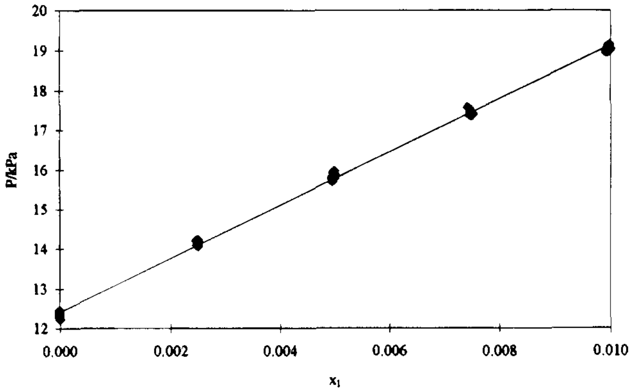

Figure 3. Pressure vs composition curve of a set of experimental simulation results: (◆) simulated Experimental Data; (—) first-order polynomial.

sets the two intensive variables, temperature and density. The phase rule is satisfied.

A constant temperature, constant volume flash using the current estimate for the infinite dilution behavior is incorporated into the data analysis. The true phase behavior is not known at this low composition. Consequently, this is an iterative process. The data analysis begins by assuming that the liquid composition is equal to the bulk composition. A weighted regression analysis provides an estimate of the limiting slope. This provides the initial estimate of γ_1^∞. The UNIQUAC solution model parameters are estimated using the estimated value of γ_1^∞ and a literature value for γ_2^∞. The flash provides revised estimates for x. The process is repeated until the estimate for γ_1^∞ stops changing.

This experimental method and data analysis method present two possibly significant systematic errors in the estimate for γ_1^∞. First, the estimate is dependent upon the literature estimate for γ_2^∞. There is the potential that if the value is grossly in error, the estimate for γ_1^∞ will be biased. Second, the solution model used for the interpolation, UNIQUAC in this case, may not properly represent the phase behavior. These two possibilities along with others can be evaluated using appropriate experimental design hypotheses.

Experimental Design

In addition to the significant questions of systematic errors, additional questions concerning the extrapolation form to estimate the limiting slope, the number of data points, the values for the bulk compositions, and the effects of experimental errors needed to be resolved to evaluate the accuracy and precision of the resultant γ_1^∞. The method of Howat and Swift (1983) was used to evaluate the possible experimental designs and the possible analysis methods and to minimize the measurement effort.

Figure 3 shows a sample graph of pressure versus liquid composition produced from a simulation run. The pseudo-experimental data are analyzed using one of the possible procedures for extrapolating the results to zero solute concentration, and a value of γ_1^∞ is obtained. This value is compared to the "true" value of γ_1^∞ to determine the error in this experimental run. The experiment design evaluation is repeated several times to find the average, deviation, and bias of γ_1^∞ resulting from that specific experimental design.

Table 1 presents a summary of the experimental design results used to evaluate the method and design of the equipment. The following presents a discussion focused on addressing specific questions. Tiegs et al. (1986) states that it is difficult to evaluate the effect of the extrapolation on the error in the estimate of the infinite dilution activity coefficient. The experimental design results attempt to quantify this error in the form of a total error function:

$$\delta^2_{\mathrm{total}} = \delta^2_{\mathrm{bias}} + \delta^2_{\mathrm{random}} \tag{4}$$

where δ_{bias} is the difference between the canonical value of γ_1^∞ and the calculated value of γ_1^∞. δ_{random} is the sample standard deviation of γ_1^∞.

The Appendix gives the physical properties and model equations used during the experimental design analysis.

1. Which of the Extrapolating Methods Provides the "Best" Estimate for γ_1^∞? Equation 3 was found to be highly linear for acetone + water. It produced the best value of the infinite dilution activity coefficient when the same canonical data set was analyzed using the methods described in the previous section. For this reason eq 3 is used as the basis of this work.

A first- or second-order polynomial fit of pressure versus composition proved to introduce, respectively, a large bias and large random error. A straight line does not describe the P vs x_1 data; the data follow a slight curve. The slope of the regressed line is therefore an average slope over a larger composition, and not the slope at $x_1 = 0$. This gave consistently low values for γ_1^∞. Taking lower compositions over a smaller, more linear range was tried without success, as explained in section 4, below. A second-order polynomial was then tried, but the derivative of this curve fit (the linear coefficient) was highly uncertain. The average was very close to the canonical value of γ_1^∞, indicating this method introduced little bias, but the sample standard deviation was very large, giving a large random error in γ_1^∞.

Section A of Table 1 summarizes the simulations run in order to answer this question. The three curve-fitting functions used were a first-order polynomial fit of the P vs x_1 curve, a second-order polynomial fit of the P vs x_1 curve, and a first-order fit of the pressure departure (P_d) function of Ellis and Jonah (1962) divided by x_1x_2 (herein referred to as the P_d analysis method). In these cases four points were taken at values of x_1 from 0 to 0.004 mole fraction. The $x_1 = 0$ point represents a vapor pressure reading that was included in the maximum likelihood regression of the fitting curve. (The P_d analysis requires fitting a line through the P_d/x_1x_2 equation, so the zero composition point cannot be directly included in the regression. The vapor pressure is used implicitly in the definition of P_d, however, so that the vapor pressure information does not go unused. Maher and Smith (1979) show that the P_d analysis is equivalent to a third-order polynomial fit of the $P-x$ data). These three cases demonstrate that, over this range of compositions, the straight line fitting equation introduced significant bias but reasonable random error, while the two more complex fitting equations produced very little bias, but increased the random error dramatically. The value of $(\partial P/\partial x_1)_{x=0}$ is not well represented by an overall average slope; in general, the magnitude of the slope increases as the curve nears $x_1 = 0$. A second-order curve takes this into account, and the P_d analysis changes the function entirely, so that the bias caused by assuming the overall slope is equal to the slope at zero is done away with. However, the random error is magnified in taking the derivative of the second-order function or in dividing P_d by x_1. This effect is most dramatically seen in the P_d function as $x_1 \rightarrow 0$, as shown in Figure 5.

2. How Much Systematic Error Is Introduced by Using UNIQUAC for the Interpolation Formula To Estimate the P−x Relationship? Conclusions drawn

Table 1. Experimental Design Summary

	error					x_1			
γ_1^∞	random	bias	total	curve fit	no. of points	initial	final	no. of repeats	pertinent factors in simulation run
					A. Curve Fitting Function				
8.76	0.32	−0.26	0.41	1st	4	0.000	0.004	0	base case—straight line fit of data
9.02	1.11	0.00	1.11	2nd	4	0.000	0.004	0	2nd−order curve fit of data
9.04	1.04	0.02	1.04	P_d	4	0.001	0.004	0	P_d analysis of data
					B. Composition Range				
8.41	0.14	−0.61	0.62	1st	4	0.000	0.010	0	higher composition range, 1st order
9.00	0.46	−0.02	0.46	2nd	4	0.000	0.010	0	higher composition range, 2nd order
9.00	0.35	−0.02	0.35	P_d	4	0.004	0.010	0	higher composition range, P_d analysis
					C. Number of Points				
8.76	0.34	−0.26	0.43	1st	3	0.000	0.004	0	3 data points, normal composition
8.76	0.32	−0.26	0.41	1st	4	0.000	0.004	0	4 data points, normal composition
8.75	0.28	−0.27	0.39	1st	7	0.000	0.004	0	7 data points, normal composition
8.40	0.12	−0.62	0.63	1st	7	0.000	0.010	0	7 data points, higher composition
9.00	0.40	−0.02	0.40	2nd	7	0.000	0.010	0	7 data points, higher composition, 2nd order
9.00	0.46	−0.02	0.46	2nd	4	0.000	0.010	0	compare to 7 points, above
					D. Repeated Points				
8.75	0.24	−0.26	0.36	1st	3	0.000	0.004	1	3 × 2 repeat, 1st order
8.42	0.11	−0.60	0.61	1st	3	0.000	0.010	1	3 × 2 repeat, 1st order, high composition
9.02	0.83	0.01	0.83	2nd	3	0.000	0.004	1	3 × 2 repeat 2nd order
9.00	0.34	−0.02	0.34	2nd	3	0.000	0.010	1	3 × 2 repeat, 2nd order, high composition
9.00	0.24	−0.01	0.24	P_d	3	0.004	0.010	1	3 × 2 repeat, P_d analysis, high composition
					E. Vapor Pressure Not Included in Regression				
8.68	0.47	−0.33	0.58	1st	3	0.001	0.004	0	P^0 not included, 3 points
8.69	0.45	−0.33	0.56	1st	4	0.001	0.004	0	P^0 not included, 4 points
8.76	0.32	−0.26	0.41	1st	4	0.000	0.004	0	base case, P^0 included
					F. Different Solution Model Used as Canonical Model				
11.0	0.33	−0.51	0.61	1st	4	0.000	0.004	0	Wilson model used, gamtrue = 11.570
11.5	0.46	−0.05	0.47	2nd	4	0.000	0.010	0	Wilson model used, gamtrue = 11.570
11.5	0.48	−0.05	0.49	2nd	3	0.000	0.010	0	Wilson model used, gamtrue = 11.570
					G. Value of γ_2^∞ Changed				
8.75	0.34	−0.27	0.43	1st	3	0.000	0.004	0	$\gamma_2^\infty = 1.50$
8.75	0.32	−0.26	0.41	1st	4	0.000	0.004	0	$\gamma_2^\infty = 4.4$
8.76	0.32	−0.26	0.41	1st	4	0.000	0.004	0	$\gamma_2^\infty = 5.45$
8.75	0.32	−0.27	0.42	1st	4	0.000	0.004	0	$\gamma_2^\infty = 6.6$
8.76	0.34	−0.26	0.42	1st	3	0.000	0.004	0	$\gamma_2^\infty = 10.9$

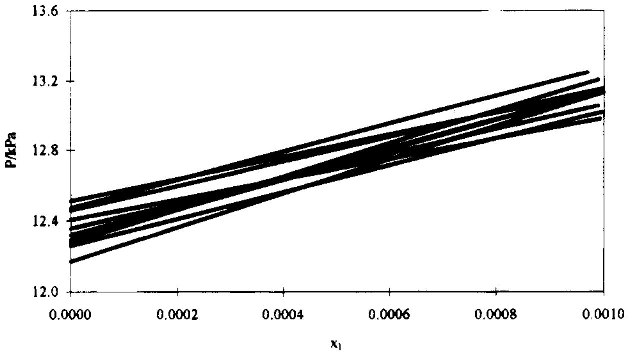

Figure 4. Experimental simulation data at very low compositions: (—) examples of first-order polynomials resulting from simulated experiments.

from Monte Carlo experimental design methods can be biased when the underlying model used to generate the true behavior is also used in the analysis of the simulated data. In this case, UNIQUAC was used to generate the true behavior and to describe the flash. In the real world the model used to describe the flash will not exactly match the true form of the phase behavior. This potential bias can be evaluated by using an entirely different solution model to generate the canonical data while still using the UNIQUAC equation to evaluate the flash. The Wilson equation was used as the canonical model with parameters selected to give results dramatically different from those of the UNIQUAC canonical model. Section F of Table 1 provides a summary of this evaluation. The bias introduced by using the Wilson equation determined from the "experiment" is larger than in the previous case, but only slightly so. The data evaluation method actually gave slightly better percentage results when the data were evaluated using a second-order polynomial curve. The bias introduced by applying a different model to the true underlying data is much smaller than the random error caused by experimental measurements.

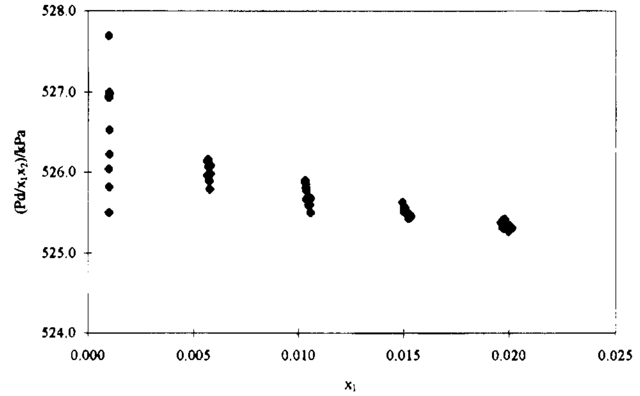

Figure 5. Experimental simulation data analyzed with the P_d function of Ellis and Jonah (1962): (◆) simulated experimental data in P_d format.

3. How Much Systematic Error Is Introduced by Using the Literature Estimate for γ_2^∞? Group G in Table 1 shows that the impact of the value of γ_2^∞ has very little influence upon the estimate for γ_1^∞. The value of γ_2^∞ was increased by 100% and decreased to half its value without appreciably changing the resultant value of γ_1^∞. The binary interaction parameters of the solution model are representative of the interaction energy of the infinitely

Table 2. Experimental Vapor Pressure Measurements

chemical	T/K	P^{exp}/kPa	$P^{\text{lit.}}$/kPa
acetone	317.70	66.59	67.23
acetone	317.72	66.90	67.27
water	317.72	9.36	9.37
water	317.78	9.55	9.41

dilute species with the solvent, and one end has a minimal impact on the other end of the mixture composition.

4. What Is the Impact of the Bulk Compositions Used in the Experiment, i.e., What is the Relation between Low Compositions and the Experimental Metering and Pressure Error? The pressure versus composition curve can be well represented by a line over a very small range of compositions. Unfortunately, this region is so small that pressure differences from point to point are smaller than the accuracy of the pressure transducer and slopes of the P vs x_1 curve are widely scattered, resulting in large random errors regardless of the fitting function. This wide scatter is seen in Figure 4 which presents first-order descriptions of the simulated $P-x$ relationship. Terminating the experiment with larger compositions tends to result in $P-x$ curvature which cannot be described well with a first-order polynomial. This will bias the estimate of γ_1^∞, as can be seen in comparing line 1 of section A with line 1 of section B in Table 1. The bias introduced using a second-order polynomial or P_d analysis does not change significantly. This indicates they can better represent the data over larger ranges of composition. Another result of larger compositions is that the relative errors in both pressure measurement and composition measurement are reduced, so the data are less scattered, resulting in smaller random error for all three methods.

5. What Is the Impact on the Estimate for γ_1^∞ As the Number of Measurements Increases? The number of data points used was another key design parameter. Group C designs in Table 1 show that four experimental points is satisfactory. Increasing the number of points to seven does not markedly affect the random or bias errors.

6. What Is the Impact of Replicating Experiments Compared with Additional, New Compositions on the Total Error in the Estimate for γ_1^∞? Results in section D of Table 1 show that it is more advantageous to replicate the experiment with few points than to extend a data set by the same number of points. For example, compare the fourth entry of section D with the fifth entry of section C. The composition span, initial composition, and method of $P-x_1$ description are the same. The latter contains one more experimental point than the design in section D. Note, however, that the random error is reduced by replicating the three-point design instead of adding points to the design.

7. What Is the Impact of Including the Experimental Vapor Pressure for the Solvent on the Estimate of γ_1^∞? The vapor pressure of the solvent is also an important point to use in the regression. It has no error associated with composition, only with pressure and temperature measurement. It tends to reduce both bias and random error and should most definitely be used as seen in section E of Table 1.

Verification of the Technique Using Experimental Data

The vapor pressure measurements of acetone and water are shown in Table 2. These data were compared to literature-based vapor pressure correlations (see the Appendix). Estimated values based on this correlation are shown as $P^{\text{lit.}}$ in the table. Vapor pressures for acetone are taken from Boublik and Aim (1972), Ambrose et al. (1974), and Brown and Smith (1957). Vapor pressures for water were taken from Osborn and Douslin (1974) and Douslin and Osborn (1965). Critical properties are taken from Reid et al. (1987). The water vapor pressure measurements are in agreement with literature values while acetone vapor pressure measurements are more than 2 standard deviations below literature values. This is somewhat troubling, but experimental design shows the experimental method for finding infinite dilution activity coefficients to be insensitive to the vapor pressure of the solute.

Table 3. Experimental $T-P-z$ Measurements[a]

T/K	P/kPa	z_1	x_1
317.70	10.2	0.0017	0.0017
317.69	12.3	0.0053	0.0053
317.71	14.6	0.0104	0.0103
317.75	17.2	0.0154	0.0154
317.78	10.4	0.0017	0.0016
317.81	12.2	0.0054	0.0050
317.79	14.7	0.0104	0.0097
317.77	17.0	0.0154	0.0144

[a] Volume is fixed at 10.20 cm^3.

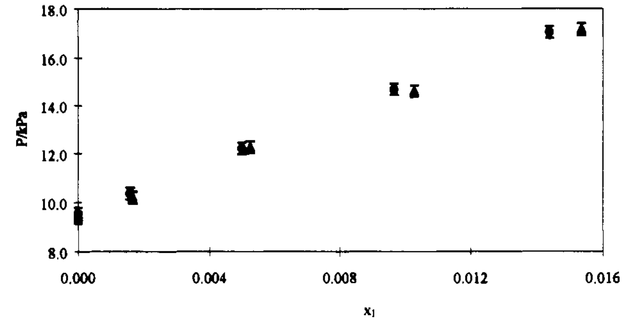

Figure 6. Experimental pressures at varying liquid mole fractions: (▲) 310.70 K; (●) 317.80 K.

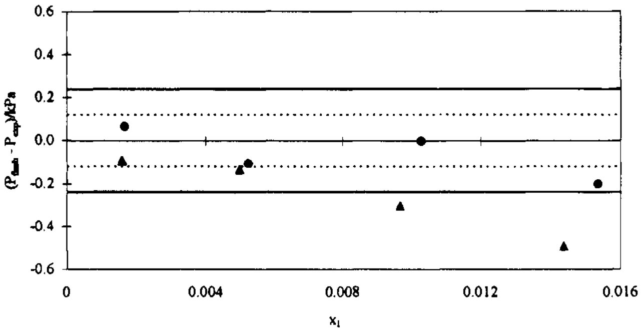

Figure 7. Pressure residuals between experimental data and flash prediction: (▲) 310.70 K; (●) 317.80 K; (···) 67% confidence interval; (—) 95% confidence interval.

Experimental $T-P-z$ measurements are listed in Table 3 and shown graphically in Figure 6. The temperature, volume, and moles of each species are fixed, effectively setting the temperature and molar volume as the independent variables. Pressure is a dependent variable. The UNIQUAC solution model is used to compare the experimental pressure against the pressure predicted from the flash calculation. These pressure residuals are plotted in Figure 7. This figure shows that two of the experimental points lie outside the acceptable region and should be given special consideration when using these data to draw a conclusion. In this work these data were used, but only along with a replicate data set.

The quantity $(\partial P/\partial x_1)_{x=0}$ must be obtained by extrapolation from finite regions to zero composition. The experi-

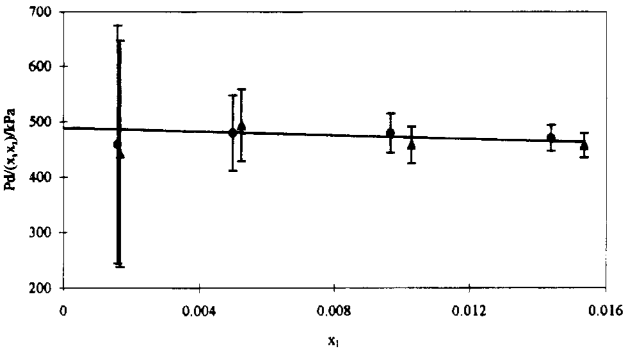

Figure 8. Experimental data subject to P_d analysis of Ellis and Jonah (1962): (▲) 310.70 K; (●) 317.80 K; (—) weighted regression.

Table 4. Experimental Results and Literature Survey

T/K	γ_1^∞	source
317.75	8.3 ± 0.1	this work
313.15	8.20	Shaw and Anderson (1983)
313.15	8.90	Hofstee et al. (1960)
318.15	8.99	Lee (1983)

mental design has shown that the best method for extrapolating to zero composition is to transform the data into the form of eq 2 and regress a weighted least-squares line through these data. The experimental data subject to this treatment are shown in Figure 8.

The intercept of the regression line provides a value of $\partial P/\partial x_1$ of 546.2 kPa. From this limiting slope an estimate of γ_1^∞ of 8.3 was obtained. Statistical analysis provides an estimate of the error of the intercept of this line which translates into an uncertainty in the value of γ_1^∞ of ±0.1.

The experimentally obtained value of γ_1^∞ is compared with values of γ_1^∞ near this temperature drawn from the literature. These values are shown in Table 4.

The data from the literature are scattered and show relatively large differences. As a result it is impossible to state that our estimate agrees with all literature values since the literature values themselves are not consistent. Our results are statistically the same as those of Shaw and Anderson (1983), but not those of Hofstee et al. (1960) and Lee (1983).

Conclusions and Recommendations

An experimental method employing a modified static cell device for measuring infinite dilution activity coefficients of volatile organic compounds in water has been developed. The equipment employs a large, calibrated vapor space to minimize the effect of noncondensable chemicals on the pressure measurement. A data analysis method corrects the liquid composition to account for the volatile organic compound present in the vapor space. The suitability of the equipment and method has been verified using experimental design techniques. They are further supported by experimental results for the acetone + water system.

Nomenclature

A,B,C,D	Miller vapor pressure equation coefficients
l	parameter in eqs A-2
P	total pressure
P^0	vapor pressure
ΔP	pressure departure function
q	UNIQUAC pure component parameter
r	UNIQUAC pure component parameter
T	temperature
$u_{ji}-u_{ii}$	binary interaction parameter used in the UNIQUAC solution model
V^*	characteristic volume used in the liquid molar volume correlation, L/mol
x	liquid-phase composition (mole fraction)
y	vapor-phase composition (mole fraction)
z	overall composition (mole fraction)
γ	activity coefficient
γ^∞	activity coefficient at infinite dilution
θ	parameter in eqs A-2
Φ	parameter in eqs A-2
τ	interaction parameter in the UNIQUAC model, eqs A-2
ω_{SRK}	acentric factor used in the liquid molar volume correlation

Subscripts

c	value at the critical point
i	component in a mixture, general
j	component in a mixture, general
k	component in a mixture, general
1	component 1 of a mixture, usually acetone
2	component 2 of a mixture, usually water

Superscripts

C	combinatorial contribution to the activity coefficient, eqs A-2
R	residual contribution to the activity coefficient, eqs A-2.
∞	at infinite dilution conditions

Appendix

The vapor pressures found were used with vapor pressures and critical properties taken from the literature and correlated using the full-range vapor pressure equation of Miller (1964):

$$P_i^0/\mathrm{kPa} = \exp(A_i/(T/\mathrm{K}) + B_i + C_i(T/\mathrm{K}) + D_i(T/\mathrm{K})^2) \qquad \text{(A-1)}$$

The solution model used is the UNIQUAC model of Abrams and Prausnitz (1975):

$$\ln \gamma_i = \ln \gamma_i^{\mathrm{C}} + \ln \gamma_i^{\mathrm{R}} \qquad \text{(A-2a)}$$

$$\ln \gamma_i^{\mathrm{C}} = \ln \frac{\Phi_i}{x_i} + \frac{z}{2} q_i \ln \frac{\theta_i}{\Phi_i} + l_i - \frac{\Phi_i}{x_i} \sum_j x_j l_j \qquad \text{(A-2b)}$$

$$\ln \gamma_i^{\mathrm{R}} = -q_i \ln(\sum_j \theta_j \tau_{ji}) + q_i - q_i \sum_j (\theta_j \tau_{ij} / \sum_k \theta_k \tau_{kj}) \qquad \text{(A-2c)}$$

$$l_j = (z/2)(r_j - q_j) - (r_j - 1) \qquad \text{(A-2d)}$$

$$\theta_i = q_i x_i / \sum_j q_j x_j \qquad \text{(A-2e)}$$

$$\Phi_i = r_i x_i / \sum_j r_j x_j \qquad \text{(A-2f)}$$

$$\tau_{ji} = \exp(-(u_{ji} - u_{ii})/RT) \qquad \text{(A-2g)}$$

and note that $\tau_{ii} = \tau_{jj} = 1$.

Values of the vapor pressure coefficients, molar volume correlation coefficients for Hankinson and Thomson (1979), and solution model interaction parameters are shown in Table 5.

Table 5. Pure Component Properties and Correlation Coefficients

	acetone (1)	water (2)
vapor pressure coefficients (eq A-1)		
A	−4958.529	−6267.821
B	25.5409	26.4272
C	-2.40254×10^{-2}	-1.75385×10^{-2}
D	1.89008×10^{-5}	1.10070×10^{-5}
liquid density correlation		
$V^*/(\mathrm{m^3 \cdot mol^{-1}})$	2.080×10^{-4}	4.35669×10^{-5}
ω_{SRK}	0.3149	−0.65445
T_c (specific to correlation)/K	508.15	647.37
T_c/K	508.1	647.3
P_c/kPa	4701	22120
molecular weight	58.080	18.015
solution model canonical parameters		
$(u_{ji}-u_{ii})/(\mathrm{kJ \cdot mol^{-1}})$	3.166	−0.5773
q	2.336	1.400
r	2.5735	0.920

Literature Cited

Abbott, M. M. Low-Pressure Phase Equilibria: Measurement of VLE. *Fluid Phase Equilib.* **1986**, *29*, 193–207.

Abrams, D. S.; Prausnitz, J. M. Statistical Thermodynamics of Liquid Mixtures: A New Expression for the Excess Gibbs Energy of Partly or Completely Miscible Systems. *AIChE J.* **1975**, *21* (1), 116–128.

Ambrose, D.; Sprake, C. H. S.; Townsend, R. Thermodynamic Properties of Organic Oxygen Compounds. XXXIII. The Vapour Pressure of Acetone. *J. Chem. Thermodyn.* **1974**, *6*, 693–700.

Boublik, T.; Aim, K. *Collect. Czech. Chem. Commun.* **1972**, *37*, 3513.

Brown, I.; Smith, F. Liquid-Vapour Equilibria. *Aust. J. Chem.* **1957**, *10*, 423–428.

Douslin, D. R.; Osborn, A. *J. Sci. Instrum.* **1965**, *42*, 369.

Ellis, S. R. M.; Jonah, D. A. Prediction of Activity Coefficients at Infinite Dilution. *Chem. Eng. Sci.* **1962**, *17*, 971–976.

Gautreaux, M. F., Jr.; Coates, J. Activity Coefficients at Infinite Dilution. *AIChE J.* **1955**, *1* (4), 406–500.

Hankinson, R. W.; Thomson, G. H. A New Correlation for Saturated Densities of Liquids and Their Mixtures. *AIChE J.* **1979**, *25* (4), 653–663.

Hartwick, R. P.; Howat, C. S. The Contribution of Phase Equilibria to the Uncertainty in Volatile Organic Chemical Removal from Waste Water Using Distillation. Presented at the AIChE Mid-America Regional Student Paper Contest, Manhattan, KS, 1993.

Hofstee, M. T.; Kwantes, A.; Rijnders, C. W. A. *Proc. Int. Symp. Distill.* **1960**, *105* 1060. as found in Tiegs et al. (1986).

Howat, C. S. *Phase Equilibrium Studies of the Isoprene, n-Pentane, Cyclopentadiene and Dicyclopentadiene System from 290 to 360 K.* Ph.D. Dissertation, University of Kansas, Lawrence, KS, 1983.

Howat, C. S.; Swift, G. W. A Procedure for the Design of Experiments in Fluid Phase Equilibria. *Fluid Phase Equilib.* **1983**, *14*, 289–301.

Howat, C. S.; and Swift, G. W. Vapor-Liquid Phase Equilibria for the Isoprene-n-Pentane Binary System from 300 to 330K. *Fluid Phase Equilib.* **1984**, *21*, 113–134.

Laird, D. G.; Howat, C. S. Vapor-Liquid Phase Equilibria and Molar Volumes of the Butadiene-Acetonitrile System from 300 to 335K. *Fluid Phase Equilib.* **1990**, *60*, 173–190.

Lee, H. J. *Hwahak Konghak* **1983**, *21*, 317 as found in Tiegs et al. (1986).

Leroi, J. C.; and Masson, J. C. Accurate Measurement of Activity Coefficients at Infinite Dilution by Inert Gas Stripping and Gas Chromatography. *Ind. Eng. Chem. Process Des. Dev.* **1977**, *16* (1), 139–144.

Maher, P. J.; Smith, B. D. Infinite Dilution Activity Coefficient Values from Total Pressure VLE Data. Effect of Equation of State Used. *Ind. Eng. Chem. Fundam.* **1979**, *18* (4), 354–357.

Osborn, A. G.; Douslin, D. R. Vapor-Pressure Relations for 15 Hydrocarbons. *J. Chem. Eng. Data* **1974**, *19*, 114–117.

Reid, R. C.; Prausnitz, J. M.; Poling, B. *The Properties of Gases and Liquids*, 4th ed.; McGraw-Hill: New York, 1987.

Rogalski, M.; Malanowski, S. Ebulliometers Modified for the Accurate Determination of Vapour-Liquid Equilibrium. *Fluid Phase Equilib.* **1980**, *5*, 97–112.

Shanker, G.; Howat, C. S., III; Torres, R. R.; Swift, G. W. Vapor-Liquid Equilibria for 2-Methyl-1-butene and 2-Methyl-1,3-butadiene at 310.93, 316.48, and 323.03K. *Fluid Phase Equilib.* **1981**, *5*, 305–321.

Shaw, D. A.; Anderson, T. F. Use of Gas Chromatographic Headspace Analysis in Vapor-Liquid Equilibrium Data Collection. *Ind. Eng. Chem. Fundam.* **1983**, *22*, 79–83.

Tiegs, D.; Gmehling, J.; Mediva, A.; Soares, M.; Bastos, J.; Alessi, P.; Kikic, I. *Activity Coefficients at Infinite Dilution*; DECHEMA Chemistry Data Series; DECHEMA: Frankfurt/Main, Germany, 1986; Vol. IX, Parts 1–4.

Tomlins, R. P.; Marsh, K. N. A New Apparatus for Measuring the Vapour Pressure of Liquid Mixtures. Excess Gibbs Free Energy of Octamethylcyclotetrasiloxane + Cyclohexane at 308.15K. *J. Chem. Thermodyn.* **1976**, *8*, 1185–1194.

Received for review November 14, 1994. Accepted March 23, 1995.[⊗] The authors acknowledge the generous contributions to the Kurata Thermodynamics Laboratory by the Occidental Petroleum Foundation for partial support of R.P.H.

JE940242C

[⊗] Abstract published in *Advance ACS Abstracts,* June 1, 1995.